SHEM: An optimal coarse space for RAS and its multiscale approximation

Martin J. Gander[1] and Atle Loneland[2]

1 Introduction and Model Problem

Domain decomposition methods for elliptic problems need a coarse space component in order to be scalable, and there are many now classical results in the literature on such two level Schwarz, balancing Neumann-Neumann and FETI methods, see [20] and references therein. Coarse spaces can however do much more for a subdomain iteration than just make it scalable. For each domain decomposition method, there exists an optimal coarse space which will make it converge in only one iteration, i.e. makes the method into a direct solver. A first such coarse space component was discovered within transmission conditions in [12]. A separate optimal coarse space was developed in [9], and also introduced in [11], with easy to use approximations to get practical coarse spaces, see also [10] where the case of discontinuous subdomain iterates was treated. The full potential of these new coarse spaces for additive Schwarz methods (AS) applied to multiscale problems was realized in [13], where also a convergence analysis can be found.

We explain here what this optimal coarse space is for Restricted Additive Schwarz (RAS). RAS was discovered in [2], and it represents a consistent discretization of the parallel Schwarz method that was introduced by Lions in the first DD conference [16], see [5] and [8] for more explanations. There is no general convergence theory for RAS, but the results of Lions apply in the discrete setting. The optimal coarse space and its approximation also differ from the case of AS, since RAS iterates are in general discontinuous.

Our approximations of the optimal coarse space are related to more recent developments of robust coarse spaces for high contrast problems, see [1] and the analysis in [14], where multiscale finite elements were proposed for the

Section of Mathematics, University of Geneva, 1211 Geneva 4, Switzerland Martin.Gander@unige.ch · Department of Informatics, University of Bergen, 5020 Bergen, Norway Atle.Loneland@ii.uib.no

coarse space. The idea to enrich the coarse space goes back to [6] and [7], where subdomain eigenfunctions are combined with partition of unity functions, see also [4]. A different approach is using eigenfunctions of the Dirichlet to Neumann map of each subdomain, see [3], the improved variant based on a generalized eigenvalue problem in the overlaps in [19], and also the recent adaptive coarse spaces for BDD(C) and FETI(-DP) methods [17, 15]. A good overview of the most recent approaches can be found in [18]. The main difference in our approach is that we start with an optimal coarse space depending on the method for which we want to construct the coarse space, and that we do not need volume eigenproblems in our construction.

Our model problem is the elliptic boundary value problem

$$-\nabla \cdot (\alpha(x)\nabla u) = f \text{ in } \Omega, \quad u = 0 \text{ on } \partial\Omega, \tag{1}$$

where Ω is a bounded convex domain in $\mathbb{R}^2$, $f \in L^2(\Omega)$ and $\alpha \in L^\infty(\Omega)$ such that $\alpha \geq \alpha_0$ for some positive constant α_0. Discretizing this problem using a P1 finite element method leads to the linear system

$$A\mathbf{u} = \mathbf{f}. \tag{2}$$

Based on a decomposition of the domain Ω into J non-overlapping subdomains $\widetilde{\Omega}_j$, which are enlarged to create overlapping subdomains Ω_j, one can construct non-overlapping restriction matrices $\widetilde{R}_j$, associated overlapping restriction matrices R_j, and local subdomain matrices $A_j := R_j A R_j^T$ to define RAS,

$$\mathbf{u}^{n+1} = \mathbf{u}^n + \sum_{j=1}^{J} \widetilde{R}_j^T A_j^{-1} R_j(\mathbf{f} - A\mathbf{u}^n), \tag{3}$$

see [2], and [5, 8] for more details.

2 Optimal Coarse Space

To discover the optimal coarse space for RAS, we define the error $\mathbf{e}^n := \mathbf{u} - \mathbf{u}^n$ and look at properties of the error after one iteration. First note that the solution satisfies (3) at the fixed point, i.e.

$$\mathbf{u} = \mathbf{u} + \sum_{j=1}^{J} \widetilde{R}_j^T A_j^{-1} R_j(\mathbf{f} - A\mathbf{u}). \tag{4}$$

Taking the difference between (4) and (3), and using that for any vector $\mathbf{e}^0$ we have $\mathbf{e}^0 = \sum_{j=1}^{J} \widetilde{R}_j R_j \mathbf{e}^0$ by the definition of R_j and $\widetilde{R}_j$, we obtain

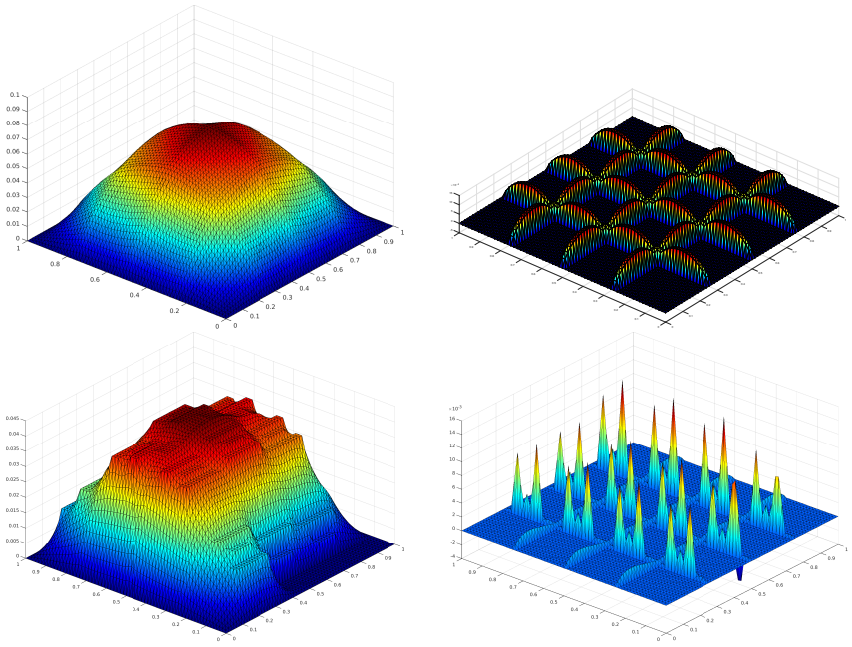

Fig. 1 Error (left) and residual (right) of the 1-level method with minimal overlap h after one iteration for the Poisson problem in the top row, and for the high contrast problem from Figure 2 on the left in the bottom row.

$$\begin{aligned}\mathbf{e}^1 &= \mathbf{e}^0 - \sum_{j=1}^{J} \widetilde{R}_j^T A_j^{-1} R_j A \mathbf{e}^0 = \sum_{j=1}^{J} \widetilde{R}_j^T A_j^{-1} A_j R_j \mathbf{e}^0 - \sum_{j=1}^{J} \widetilde{R}_j^T A_j^{-1} R_j A \mathbf{e}^0 \\ &= \sum_{j=1}^{J} \widetilde{R}_j^T A_j^{-1} (A_j R_j - R_j A) \mathbf{e}^0 = \sum_{j=1}^{J} \widetilde{R}_j^T A_j^{-1} (R_j A R_j^T R_j - R_j A) \mathbf{e}^0 \\ &= \sum_{j=1}^{J} \widetilde{R}_j^T A_j^{-1} R_j A (R_j^T R_j - I) \mathbf{e}^0.\end{aligned}$$

Now since $(R_j^T R_j - I)\mathbf{e}^0$ contains only non-zero elements outside subdomain Ω_j, $A(R_j^T R_j - I)\mathbf{e}^0$ represents precisely boundary conditions for Ω_j, and thus

$$\widetilde{R}_j \mathbf{e}^1 = \widetilde{R}_j \widetilde{R}_j^T A_j^{-1} R_j A (R_j^T R_j - I) \mathbf{e}^0$$

is a discrete harmonic function on each $\widetilde{\Omega}_j$. This is illustrated in Figure 1 for the case of the Poisson equation in the top row, where we see that the error is harmonic in the $\widetilde{\Omega}_j$ on the left and on the right we show the associated residual, which is zero in each $\widetilde{\Omega}_j$, since the error is harmonic there. In the bottom row we show the corresponding results for the high contrast problem

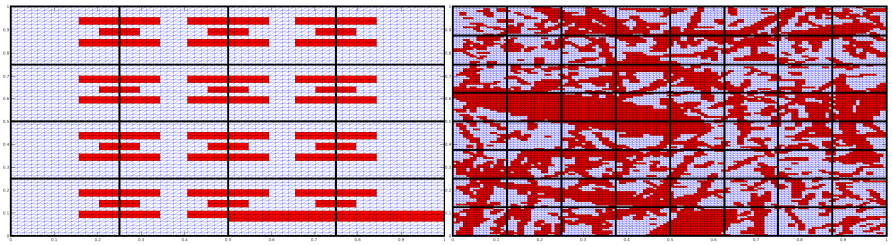

Fig. 2 Left: channel distributions of α for a geometry with $h = \frac{1}{64}$, $H = 16h$. Right: irregular distribution of α for a geometry with $h = \frac{1}{128}$, $H = 16h$.

from Figure 2 on the left, and we see that even though the error looks very different, it is still the solution of the homogeneous equation, i.e. "harmonic", in each non-overlapping subdomain, the residual is zero there.

If the coarse space should remove all of $\mathbf{e}^1$ for RAS, it needs to contain all discrete harmonic functions on each non-overlapping subdomain $\widetilde{\Omega}_j$. Putting these functions into the columns of the coarse restriction matrix R_0, the coarse correction step with $A_0 := R_0 A R_0^T$ leads to the exact solution,

$$\mathbf{u} = \mathbf{u}^1 + R_0^T A_0^{-1} R_0 (\mathbf{f} - A\mathbf{u}^1).$$

A simple basis for the optimal coarse space is to choose the functions whose value equals 1 at one node of the interface of the non-overlapping subdomains, zero at all the others, and then to harmonically extend this data inside the non-overlapping subdomain. The dimension of this optimal coarse space is thus twice the number of interface nodes of the non-overlapping decomposition, and would be infinite dimensional at the continuous level.

3 Approximation of the Optimal Coarse Space

Since the full discrete harmonic space is very large, we propose to approximate it, and it is best to explain this using as example the decomposition of the square into four sub-squares which represent the non-overlapping subdomains $\widetilde{\Omega}_j$. The first four basis functions which we put into the coarse space are shown in Figure 3 on the left. In the constant coefficient case, i.e. the Poisson equation, this would just correspond to Q1 finite elements in these square subdomains, as we see in the top row, but in the more general case of a specific distribution α as shown in Figure 2, we solve a one dimensional boundary value problem along the edges where the function is non-zero, see [13]. To get a better coarse space, we enrich the former one by adding harmonically extended eigenfunctions on each non-overlapping subdomain from an interface eigenvalue problem along each edge of the non-overlapping decom-

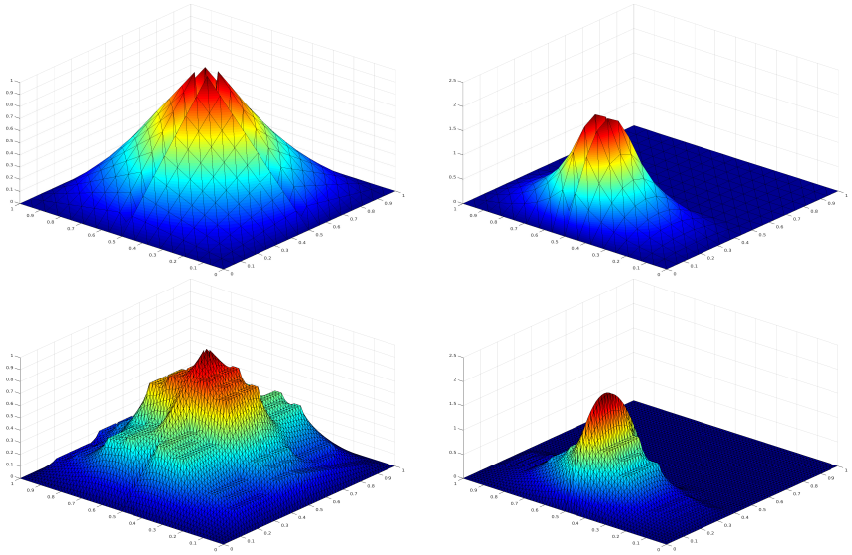

Fig. 3 Discontinuous multiscale finite element basis functions (left) and first spectral enrichment functions (right) corresponding to the Poisson case for $h = 1/32$ and $H = 16h$ in the top row, and a multiscale problem with distribution α given in Figure 2 on the left for $h = 1/64$ and $H = 32h$ in the bottom row.

position [13], which leads to the Spectral Harmonically Enriched Multiscale coarse space we call SHEM$_j$, where j indicates how many functions were added for the enrichment. An example of two such spectral coarse functions based on the first eigenfunction is shown in Figure 3 on the right for the Poisson equation on top, and below for the multiscale problem with distribution α given in Figure 2 on the left. If we add all spectral enrichment functions, we obtain again the optimal coarse space OHEM (Optimal Harmonically Enriched Multiscale coarse space).

4 Numerical Results

The first numerical experiment is for the distribution α shown in Figure 2 on the left. The iteration counts and the size of the coarse space compared to the optimal coarse space are shown in Table 1, where we run RAS or GMRES preconditioned with RAS until the l_2 norm of the initial residual is reduced by a factor of 10^6. For the solution of the generalized 1D eigenvalue problems we used `eig` in Matlab. We see that SHEM$_3$ is a robust method, independently of h, which is related to the fact that in the distribution α given in Figure 2 on the left, there are at most 3 channels crossing any one given interface. This motivates to use an adaptive variant we call SHEM$_a$, where we include

	SHEM$_3$				SHEM$_a$			
$\hat{\alpha}$	iter.	GMRES	dim.	rel. dim.	iter.	GMRES	dim.	rel. dim.
10^0	8 (8)	7 (7)	180	25% (6%)	15 (17)	10 (10)	84	12% (3%)
10^2	10 (11)	9 (9)	180	25% (6%)	15 (17)	11 (11)	132	18% (4%)
10^4	10 (11)	9 (10)	180	25% (6%)	15 (17)	12 (12)	132	18% (4%)
10^6	10 (11)	9 (10)	180	25% (6%)	15 (17)	12 (12)	132	18% (4%)

Table 1 Iteration count for RAS with the new coarse space SHEM$_3$ and SHEM$_a$ for the distribution in Figure 2 on the left, with $h = \frac{1}{64}$, $H = 16h$ and overlap $2h$ (in parenteses $h = \frac{1}{256}$, $H = 64h$ and overlap $8h$).

an adaptive number of enrichment functions on each interface, based on the size of the eigenvalues. Table 1 shows that SHEM$_a$ is also robust when the contrast increases, and uses fewer coarse functions, just a small percentage of the optimal coarse space OHEM.

We next consider the distribution of α given in Figure 2 on the right for $\hat{\alpha} = 10^4$. We show in Table 2 the iteration counts for an increasing number of coarse basis functions on each edge. For this example we consider both small overlap $\delta = 2h$ and large overlap $\delta = H$. These results show that SHEM for RAS performs very well for the fairly hard distribution of α in Figure 2 on the right. We see also that by systematically increasing the number of spectral enrichment functions on each edge we eventually reach a maximal degree where OHEM turns RAS into a direct solver, as predicted. We also note that RAS without Krylov acceleration performs about as well as RAS with GMRES when SHEM$_j$ is used with $j \geq 6$, which shows that the iterative solver is now so good that Krylov acceleration is not needed any more, a bit like multigrid for the Poisson equation.

In Table 3 we give the iteration count for the same distribution of α in Figure 2 on the right, except that we now consider an adaptive variant of the coarse space. For both small overlap $\delta = 2h$ and large overlap $\delta = H$ we consider three experiments: For the first experiment we choose the threshold for including eigenfunctions into the coarse space such that we are guaranteed that at least one spectral function is included on each subdomain edge segment. For the second experiment, the threshold is chosen such that we are guaranteed at least two spectral functions on each of the subdomain

	SHEM$_j$ $\delta = 2h$		SHEM$_j$ $\delta = H$			
j	iter.	GMRES	iter.	GMRES	dim.	rel. dim.
3	34	13	7	6	868	26%
6	9	8	5	4	1540	46%
9	7	7	4	4	2212	66%
12	6	6	4	4	2884	86%
15	1	1	1	1	3360	100%

Table 2 Iteration count for RAS with the new coarse space SHEM$_j$ for the distribution in Figure 2 on the right with $h = \frac{1}{128}$, $H = 16h$.

	SHEM$_a$ $\delta = 2h$ $(4h)$		SHEM$_a$ $\delta = H$			
min.	iter.	GMRES	iter.	GMRES	dim.	rel. dim.
1	39 (43)	20 (20)	10 (12)	7 (8)	532 (551)	16% (8%)
2	17 (21)	12 (13)	7 (7)	6 (6)	747 (782)	22% (11%)
3	13 (14)	10 (11)	6 (6)	5 (5)	980 (988)	29% (14%)

Table 3 Iteration count for RAS with SHEM$_a$ for the distribution in Figure 2 on the right with $h = \frac{1}{128}$, $H = 16h$ and overlap $2h$ (in parenteses $h = \frac{1}{256}$, $H = 32h$ and overlap $4h$).

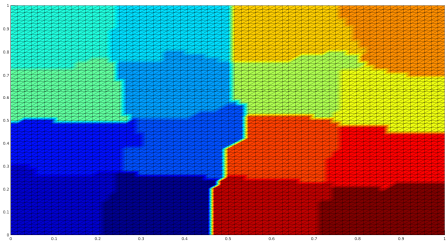

	SHEM$_0$		SHEM$_a$		
α	iter.	dim.	iter.	dim.	rel. dim.
10^0	14	49	14	49	6%
10^2	38	49	18	114	14%
10^4	92	49	12	117	15%
10^6	116	49	12	117	15%

Fig. 4 Left: Irregular decomposition of Ω into 16 subdomains with $h = 1/64$. Right: Iteration count for RAS with SHEM$_0$ and SHEM$_a$ for the distribution in Figure 2 on the left with $h = \frac{1}{64}$ and Ω subdivided as on the left, with overlap $3h$.

edge segments and for the last experiment, the threshold is chosen so that at least three spectral functions are guaranteed. The numerical results in Table 3 show that a comparable performance as the one given in Table 2 can be achieved with a considerably smaller coarse space as long as all the bad eigenmodes that are due to the discontinuities in the coefficients are included in the coarse space, and the results are similar when the mesh is refined.

We finally show a numerical experiment where we use an irregular decomposition of the domain into subdomains, as shown in Figure 4 on the left. As in the case of a regular decomposition in Figure 3, we can compute the corresponding multiscale coarse basis functions and spectral enrichment functions for each subdomain, and obtain the iteration counts in Figure 4 on the right. We clearly see that SHEM also works very well for an irregular domain decomposition, and just enriching the coarse space with the adaptively chosen number of spectral enrichment functions leads to a robust solver.

5 Conclusions

We presented an optimal coarse space for RAS called OHEM, which leads to convergence of RAS in one iteration, both when used as an iterative solver and as a preconditioner for GMRES. We then proposed an approximation called SHEM based on multiscale finite elements in each subdomain, enriched with spectral harmonic functions. We showed numerically that SHEM is robust for problems with high contrast, and also derived an adaptive variant.

References

1. J. Aarnes and T.Y. Hou. Multiscale domain decomposition methods for elliptic problems with high aspect ratios. *Acta Math. Appl. Sin. Engl. Ser.*, 18(1):63–76, 2002.
2. X.-C. Cai and M. Sarkis. A restricted additive Schwarz preconditioner for general sparse linear systems. *SIAM J. Sci. Comput.*, 21(2):792–797, 1999.
3. V. Dolean, F. Nataf, R. Scheichl, and N. Spillane. Analysis of a two-level Schwarz method with coarse spaces based on local Dirichlet-to-Neumann maps. *Comput. Methods Appl. Math.*, 12(4):391–414, 2012.
4. Y. Efendiev, J. Galvis, R. Lazarov, and J. Willems. Robust domain decomposition preconditioners for abstract symmetric positive definite bilinear forms. *ESAIM Math. Model. Numer. Anal.*, 46(5):1175–1199, 2012.
5. E. Efstathiou and M.J. Gander. Why restricted additive Schwarz converges faster than additive Schwarz. *BIT*, 43:945–959, 2003.
6. J. Galvis and Y. Efendiev. Domain decomposition preconditioners for multiscale flows in high-contrast media. *Multiscale Model. Simul.*, 8(4):1461–1483, 2010.
7. J. Galvis and Y. Efendiev. Domain decomposition preconditioners for multiscale flows in high contrast media: reduced dimension coarse spaces. *Multiscale Model. Simul.*, 8(5):1621–1644, 2010.
8. M.J. Gander. Schwarz methods over the course of time. *Electron. Trans. Numer. Anal.*, 31:228–255, 2008.
9. M.J. Gander and L. Halpern. Méthodes de décomposition de domaine. *Encyclopédie électronique pour les ingénieurs*, 2012.
10. M.J. Gander, L. Halpern, and K. Santugini. Discontinuous coarse spaces for DD-methods with discontinuous iterates. In *Domain Decomposition Methods in Science and Engineering XXI. Springer LNCSE*, pages 607–616. Springer, 2014.
11. M.J. Gander, L. Halpern, and K. Santugini. A new coarse grid correction for RAS/AS. In *Domain Decomposition Methods in Science and Engineering XXI. Springer LNCSE*, pages 275–284. Springer, 2014.
12. M.J. Gander and F. Kwok. Optimal interface conditions for an arbitrary decomposition into subdomains. In *Domain Decomposition Methods in Science and Engineering XIX*, pages 101–108. Springer, 2011.
13. M.J. Gander, A. Loneland, and T. Rahman. Analysis of a new harmonically enriched multiscale coarse space for domain decomposition methods. *arXiv preprint arXiv:1512.05285*, 2015.
14. I.G. Graham, P.O. Lechner, and R. Scheichl. Domain decomposition for multiscale PDEs. *Numer. Math.*, 106(4):589–626, 2007.
15. A. Klawonn, P. Radtke, and O. Rheinbach. FETI-DP methods with an adaptive coarse space. *SIAM J. Num. Anal.*, 53(1):297–320, 2015.
16. P.-L. Lions. On the Schwarz alternating method. I. In *First international symposium on domain decomposition methods for partial differential equations*, pages 1–42. Paris, France, 1988.
17. J. Mandel and B. Sousedík. Adaptive coarse space selection in the BDDC and the FETI-DP iterative substructuring methods: optimal face degrees of freedom. In *Domain Decomposition Methods in Science and Engineering XVI*, pages 421–428. Springer, 2007.
18. R. Scheichl. Robust coarsening in multiscale PDEs. In *Domain Decomposition Methods in Science and Engineering XX*, volume 91 of *Springer LNCSE*, pages 51–62. Springer Berlin Heidelberg, 2013.
19. N. Spillane, V. Dolean, P. Hauret, F. Nataf, C. Pechstein, and R. Scheichl. Abstract robust coarse spaces for systems of PDEs via generalized eigenproblems in the overlaps. *Numer. Math.*, 126(4):741–770, 2014.
20. A. Toselli and O. Widlund. *Domain decomposition methods—algorithms and theory*, volume 34 of *Springer Series in Computational Mathematics*. Springer-Verlag, 2005.